The role of La, Eu, Gd, and Dy lanthanides on thermoluminescence characteristics of nano-hydroxyapatite induced by gamma radiation

H. Daneshvar[1] · M. Shafaei[2] · F. Manouchehri[1] · S. Kakaei[1] · F. Ziaie[1]

Abstract

Thermoluminescence response of hydroxyapatite doped with different percentages of lanthanide elements comprises La, Eu, Gd, and Dy has been studied under the action of gamma radiation. The samples were synthesized through hydrolysis method. The irradiations were done using a ^{60}Co γ-ray source over a dose range of 25 Gy–1 kGy. The results showed that the samples have different response intensities among which mostly belonged to Dy-doped hydroxyapatite samples. The effect of dopant concentrations on the thermoluminescence intensity was also investigated. The Tm–Tstop experimental method and TLanal program were used to analyze the glow curves of the doped samples and obtain their kinetic parameters. The frequency factors and the activation energies were also obtained for different samples. The contribution of the sub-peaks was found through deconvolution procedure in the thermoluminescence responses, and the fading behaviors are also discussed. The results showed that the thermoluminescence characteristic of nanostructure hydroxyapatite sample containing 1 m% of Dy concentration has the privilege of using as a candidate for gamma radiation dosimetry.

Keywords Thermoluminescence · Lanthanide · Deconvolution · Dosimetry · Fading

1 Introduction

Thermoluminescence (TL) is one of the most frequently used techniques in radiation dosimetry for personal and environmental purposes, with outstanding success [1–4]. Many materials exhibit thermoluminescence, but some of them have already been employed as TL dosimeters. Hence, there are always interests in developing new materials which could be used for radiation dosimetry. Hydroxyapatite ($Ca_{10}(PO_4)_3(OH)_2$) is one of these materials which its TL properties were investigated by several authors [3, 5–11]. The thermoluminescence of hydroxyapatite (HAP) is particularly interesting because HAP is the main constituent of human bone, and it can be used as the bone equivalent tissue [12]. A brief review of previous studies on thermoluminescence properties of HAP can be found elsewhere [10]. According to the preceding studies, the nanostructured HAP obtained via hydrolysis method showed a single main peak at about 200 °C after gamma irradiation. It was also shown that this peak can be used for dosimetric purposes [10]. Studies on the dosimetric properties of HAP doped with rare-earth impurities are very few [10, 13–16]. Besides, doping with lanthanides is finding increased popularity nowadays as they are efficient activators for host materials in thermoluminescence application because of their unique properties. The literature survey indicated that thermoluminescent properties of hydroxyapatite with lanthanides ion had not yet been sufficiently studied. Therefore, to search for the effect of lanthanides ion on TL properties of hydroxyapatite, more work should be performed [17].

In our previous works, the TL characteristics of nanostructure HAP/Dy were studied and showed that adding of 1 mol percent (m%) of Dy to the undoped HAP, increase the TL response of the sample considerably [8]. TL properties of gamma-irradiated nanostructure hydroxyapatite

✉ F. Ziaie, fziaie@aeoi.org.ir | [1]Radiation Application Research School, Nuclear Science and Technology Research Institute, P.O. Box 11365-3486, Tehran, Iran. [2]Young Researchers and Elites Club, Science and Research Branch, Islamic Azad University, Tehran, Iran.

were also studied, and it was found that the dose responses of the HAP are strongly linear in the dose range of 25 Gy–1 kGy and saturates at a dose of 5 kGy [10]. The TL properties of micro- and nanostructure hydroxyapatite after gamma irradiation were also studied and compared. It was observed that the TL intensity of the nanostructure HAP is higher than the microstructure one [10].

In this research work, the TL characteristics of HAP doped with different dopants such as Lanthanum (La), europium (Eu), gadolinium (Gd), and dysprosium (Dy) were investigated and the variation of the obtained glow curve due to the doping of the mentioned dopants was studied. Also, the Tm–Tstop method was used to determine the number of peaks, and this was considered as the basis for TLanal software, afterward. TLanal software is developed for TL deconvolution purposes. This program can be easily implemented on Windows-based computers and can be used to analyze the first, second, general, and mixed-order kinetic parameters [18, 19].

2 Materials and methods

2.1 Sample preparation

The HAP was doped with the dopants through the hydrolysis method, and nano-powder form samples were obtained. The dopants used in this study were incorporated in their nitrate forms that were La(NO$_3$)$_2$ (Merck), Eu(NO$_3$)$_3$·6H$_2$O, Gd(NO$_3$)$_3$·6H$_2$O, Dy(NO$_3$)$_3$·6H$_2$O (Sigma-Aldrich). Calcium hydrogen phosphate dehydrate (CaHPO$_4$·2H$_2$O, DCPD) and Ca(OH)$_2$ were mixed at the (Ca + X)/P ratio of 1.67, where X is the dopant, poured into a 500 ml of 2.5 M NaOH (pH 13) and finally mixed in a high-speed agitator at 75 °C for 1 h. Then, the reaction was terminated by cooling in ice water and was subjected to filtering, washing and drying, respectively [10, 13]. The obtained powders were sintered at 900 °C for 4 h in the air [4, 20]. In order to erase any undesirable information and increase the sensitivity of the samples, it is necessary to perform a thermal treatment procedure [21]. Thus, the samples were objected to a thermal treatment at 450 °C for 2 h before irradiation.

2.2 Characterization

The phase composition was determined by XRD equipment, STOE STADI-MP diffractometer operated at 40 kV and 40 mA using Cu radiation. Scanning is carried out over the range 20° ≤ 2θ ≤ 60°. Transmission electron microscopy (TEM) studies were carried out using a Zeiss EM10C microscope at 80 kV. The specimen for TEM was prepared from the particles suspension in deionized water. A scanning

electron microscopy (SEM) system, Zeiss Company EVO 18 model, was also used in this work.

2.3 Irradiation

The samples were weighed and packed in a plastic cover. Irradiation was carried out using a ^{60}Co γ-ray source over a dose range from 25 Gy to 1 kGy at dose-rate of 2.5 Gy/s in room temperature. Corrections for the decay of the ^{60}Co radionuclide and subsequent decrease in the dose-rate were carried out.

2.4 TL reader system

The TL glow curves were recorded by a constant heating rate of 5 °C/s using a TLD reader 7102 made in Iran by Institute of Physics (IOP). The mass of all samples was approximately 50 mg, and the Tl response of each sample is mass normalized.

3 Results and discussions

3.1 Characterization

The XRD patterns of the samples are shown in Fig. 1. Evaluation and comparison of the sample diffraction patterns indicate the existence of the peaks according to the standard cards of HAP (JCPDS Card No. 00-024-0033). The patterns of doped samples are relatively similar to that of undoped HAP. SEM and TEM micrographs of the synthesized undoped HAP and also the HAP doped 1 m% of different dopants samples are demonstrated in Figs. 2 and 3, respectively. The existences of nano-size particles in the
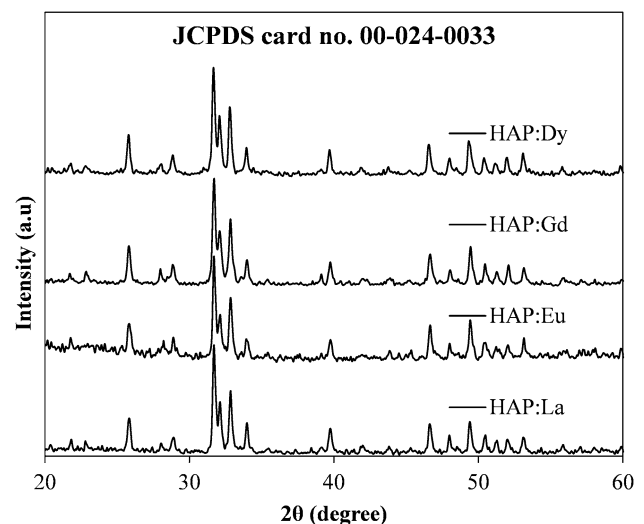

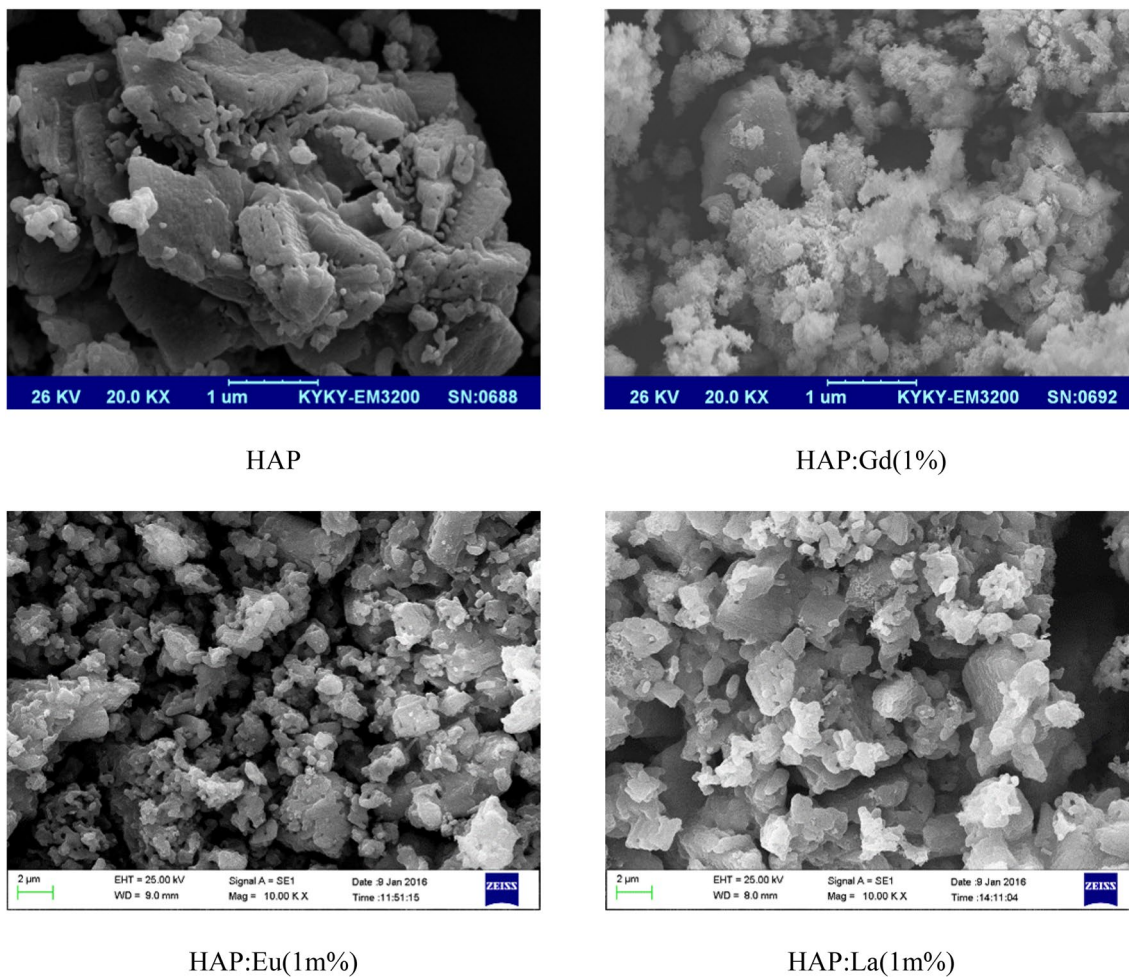**Fig. 1** XRD pattern of undoped nanostructure HAP

HAP

HAP:Gd(1%)

HAP:Eu(1m%)

HAP:La(1m%)

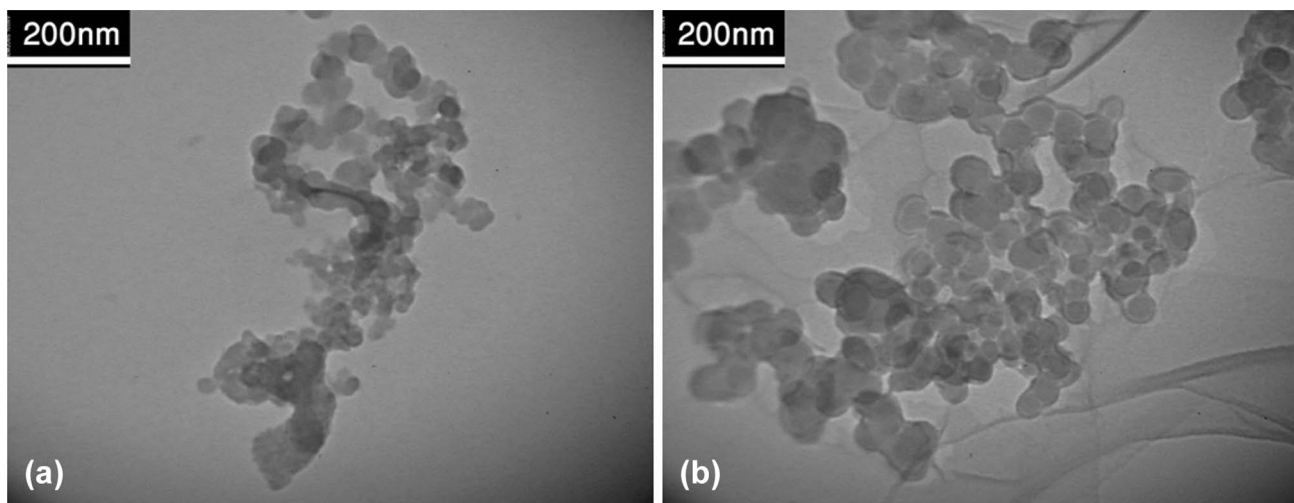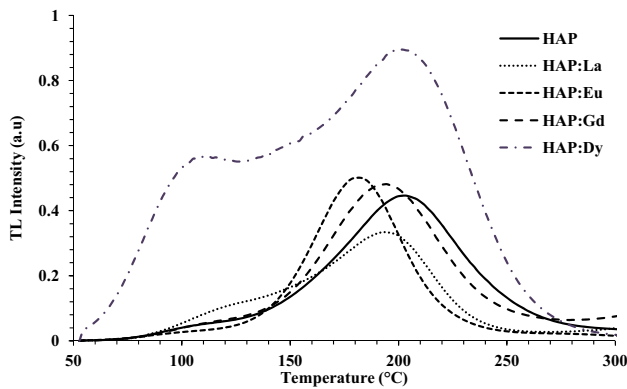**Fig. 2** SEM images of HAP doped 1 m% of different dopants

(a)

(b)

Fig. 3 TEM micrographs of **a** undoped HAP and **b** HAP:Dy (1 m%)

Fig. 4 TL glow curves of HAP doped with different elements at a concentration of 1 m% (dose = 25 Gy)

Table 1 Normalized sensitivity of main peaks for different dopants in HAP (dose = 25 Gy)

TL material	Main peak (°C)	Relative TL sensitivity (main peak height)	Relative TL sensitivity (glow peak area)
HAP	198	0.12	0.09
HAP/La	196	0.01	0.01
HAP/Eu	177	0.14	0.07
HAP/Gd	194	0.04	0.04
HAP/Dy	198	1	1

synthesized sample are obvious in the TEM images that were estimated as 10–50 nm.

3.2 Glow curve analysis

The TL glow curve of the 1 m % doped HAP samples in comparison with the undoped HAP is shown in Fig. 4. These samples were irradiated at an absorbed dose of 25 Gy. Our previous study showed that the undoped HAP has TL peaks at 115 °C and 200 °C [10]. All the glow curves of the doped samples contain two or three peaks. Apart from the Dy-doped sample, which has enhanced the main peak intensity around 200 °C, doping of Eu, La, and Gd does not have a significant effect on the peak intensities; however, peak positions have minor shifts. The TL response can be measured through both the integrating and the peak height methods which the related values are presented in Table 1. In this work, the peak height method is used for all the results. It can be observed that the glow peaks of all the samples are not located at the same temperature. This indicates that these peaks might get emerged from different traps. Among these, the Dy-doped HAP sample has the highest TL response.

The TL properties of a phosphor are appreciably influenced by trapping parameters, i.e., the order of

kinetics, trap depth, and the frequency factor. To understand the TL phenomena, knowledge of the parameter is quite important. An empirical equation has proposed to describe the TL glow peak under conditions that neither the first-order nor the second-order is satisfied. This equation is known as the general-order kinetics [22]. To determine the kinetic parameters including the peak numbers, activation energy, frequency factor, it can be used the Tm–Tstop, the initial rise, the peak shape method, and the variable heating rate methods [10]. In this study, Tm–Tstop method was used to determine the number of peaks, and then this was the basis of using TLanal Software. This method has been done for samples synthesized with dopants such as Dy, Eu, La, and Gd. In this method, samples were heated at a linear rate to Tstop temperature. Then, samples were cooled immediately to room temperature and reheated at the same rate for recording the remaining glow curve. This process was repeated several times with the same annealed/irradiated sample at different values of Tstop. The difference between the Tstop temperatures was 5 °C.

The first maximum in the glow curve was recorded. In this work, the samples were irradiated up to 800 Gy and the glow curves were recorded at 5 °C/s heating rate. These charts are shown in Fig. 5. According to this figure, each plateau region in the Tm–Tstop plot indicates the existence of an individual glow peak. There are at least 8, 6, 5, and 8 peaks in HAP nanoparticle with 1 m% dopants of La, Eu, Gd, and Dy, respectively.

Using the obtained number of peaks and their positions in this method, the sample glow curves can be deconvoluted by TLanal program. To analysis the glow curves of the doped HAP samples, the TLanal program was used for glow curve deconvolution. The kinetic parameters such as E (activation energy), s (frequency factor), and b (order of kinetics) were calculated for different peaks.

Sometimes, the first- and the second-order kinetics do not cover all possible cases of TL experimentally found kinetics [23]. May and Partridge suggested an approximate relation to describe the general-order kinetics. General-order kinetics is an interpolating function between analogous equations for first- and second-order kinetics [24]. This kinetic order can be both first- and second-order kinetics and none of the two [25]. In the first estimation for different TL materials, the general-order kinetics is used for deconvolution by software such as TLanal and TLD-MC [18, 25, 26].

To further assess the order of kinetics in our work, its position corresponding to different irradiation doses has been measured. In TL theory, the position of the first-order peak is expected to be independent of irradiation dose, whereas in second-order the position decreases with increasing of dose [27]. Figure 6 shows the peak position
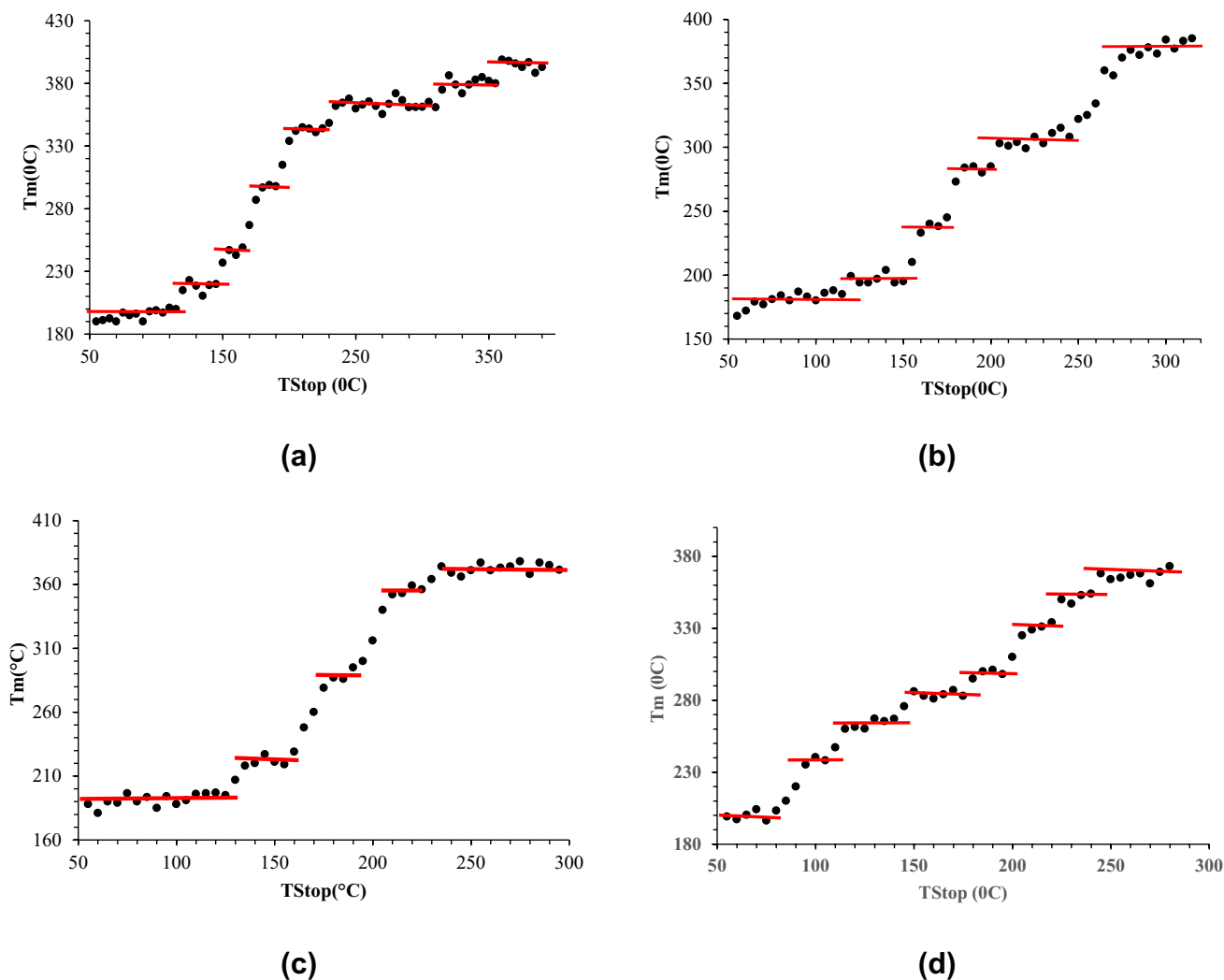
(a)

(b)

(c)

(d)

Fig. 5 Tm-Tstop charts of HAP nanoparticle with 1 m% dopants of **a** La, **b** Eu, **c** Gd, and **d** Dy
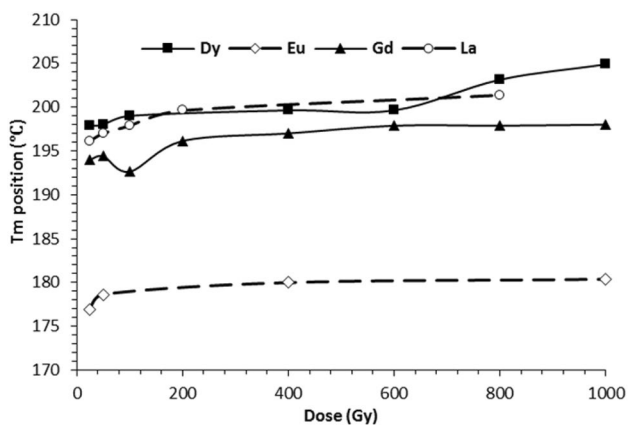

Fig. 6 Peak position as a function of dose for undoped and 1 m% doped HAP nanoparticle samples

as a function of dose for HAP nanoparticle with 1 m% dopants of La, Eu, Gd, and Dy.

Here, the maximum temperature for the main peak increases with the dose. This behavior is anomalous and cannot be accounted for exclusively by either first- or second-order. Therefore, the general-order kinetic model was used to deconvolute the glow curves of different HAP-doped samples.

The deconvoluted glow curves of the HAP doped 1 m% of dopants samples are shown in Fig. 7. All the samples are irradiated at 50 Gy of ^{60}Co gamma-ray. The number of the peaks and the associated kinetics parameters, FOM and residual standard deviation (S_{res}) calculated by the glow curve deconvolution method are given in Table 2.

As demonstrated in Fig. 7, among the peaks for each sample, some have the major contributions in the main related peak. In HAP/La (1 m%) sample, the major contributions are for the peaks located at 186 °C, 196 °C, and
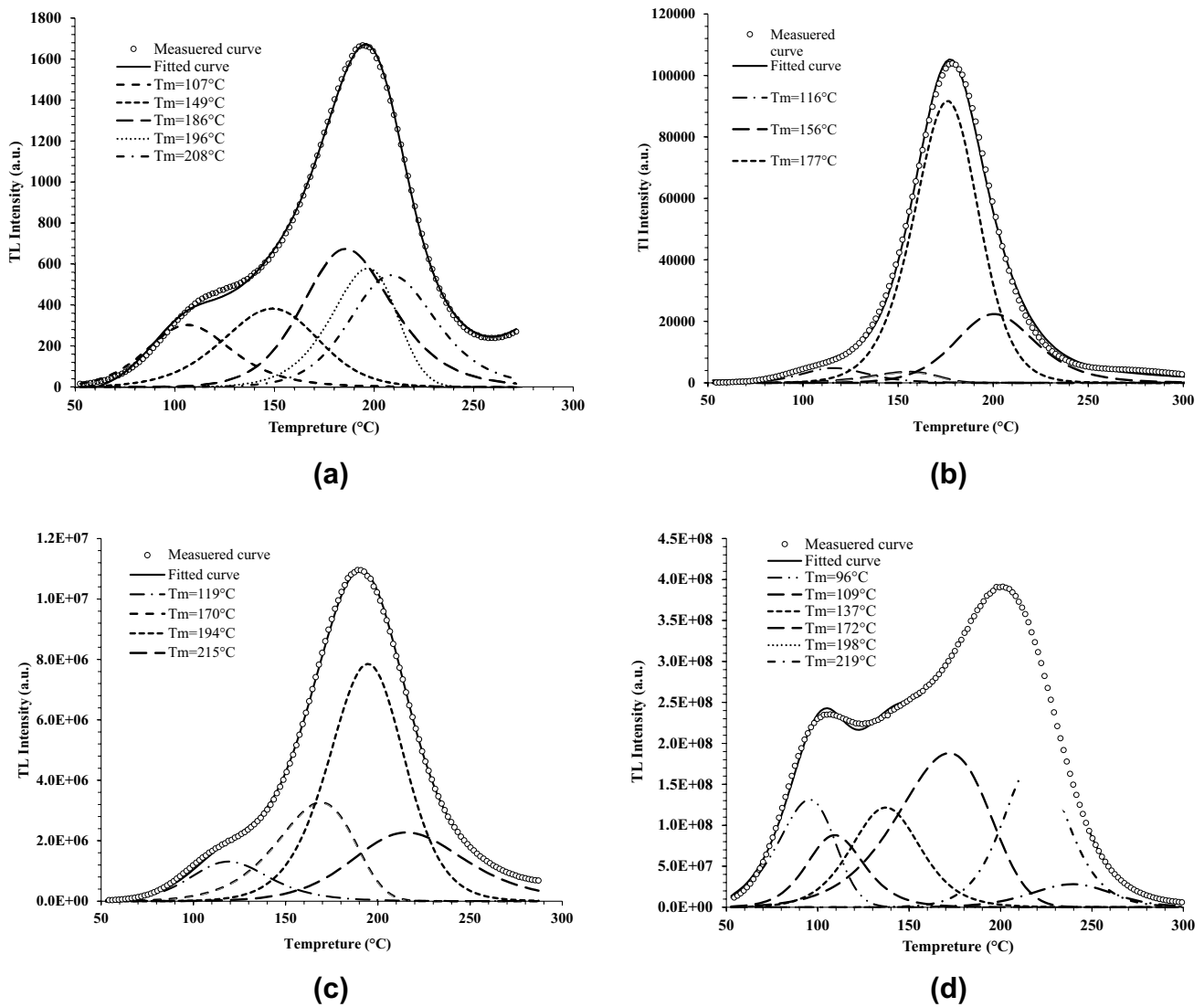
Fig. 7 Deconvoluted glow curves of HAP samples with 1 m% dopants: **a** La, **b** Eu, **c** Gd, and **d** Dy

208 °C. It is also revealed that the most intensified peak is 177 °C for HAP/Eu (1 m%), 194 °C for HAP/Gd (1 m%), and 198 °C, 172 °C, and 219 °C for HAP/Dy (1 m%).

3.3 Dose–response comparison

All the HAP-doped samples were irradiated in different doses, and their obtained glow curves were deconvoluted. The TL responses of the deconvoluted peaks versus absorbed dose for all four samples are shown in Fig. 8. As it can be seen in the figure, almost all the peak responses of the HAP/Eu and the HAP/Gd samples are saturated at doses above the 400 Gy. While, for the deconvoluted peaks of HAP/La and HAP/Dy, the approximate saturation region is about 800 Gy. Among these samples, the HAP/Dy shows a higher sensitivity in comparison with others.

The maximum number of deconvoluted peaks, 8 peaks, is observed for Dy-doped samples, as well. This indicates its complex behavior of trap structures. The TL response of the HAP-doped samples for different dopants, versus absorbed dose was also obtained and demonstrated in Fig. 9. According to this figure, the TL responses of HAP/La (1 m%) and HAP/Dy (1 m%) exhibit an almost linear response over the dose range of 25 to ~ 800 Gy. Nevertheless, for HAP/Gd (1 m%) and HAP/Eu (1 m%) samples, it can be observed in the dose range of 25 to ~ 400 Gy. On the other hand, the only dose–response of the HAP-doped Dy sample improves the undoped HAP sensitivity. Thus, the best sensitivity and response are observed for HAP doped 1 m% of Dy. This makes the Dy-doped phosphor a good candidate for TL dosimetry purposes. Some researchers reported about the role of the Dy impurity in the TL

Table 2 Kinetic parameters of the deconvoluted peaks of HAP-doped lanthanides

Sample	Peaks	T_m (°C)	s (F doss^{-1})	E (eV)	b	FOM	S_{res}
HAP/Dy (1 m%)	1	96	$2.5 \times 10^{+10}$	0.80	1.16	1.83	0.025
	2	109	$3.9 \times 10^{+14}$	1.13	1.96		
	3	137	$6.5 \times 10^{+11}$	1.00	1.73		
	4	172	$8.2 \times 10^{+06}$	0.67	1.05		
	5	198	$7.2 \times 10^{+14}$	1.43	1.98		
	6	219	$1.9 \times 10^{+16}$	1.63	1.82		
	7	240	$8.2 \times 10^{+11}$	1.27	1.59		
	8	373	$9.8 \times 10^{+05}$	0.89	2.00		
HAP/Eu (1 m%)	1	116	$2.6 \times 10^{+13}$	1.07	2.00	2.14	0.029
	2	156	$1.8 \times 10^{+10}$	0.90	1.00		
	3	177	$7.9 \times 10^{+13}$	1.28	1.56		
	4	200	$2.3 \times 10^{+13}$	1.30	2.00		
	5	261	$3.3 \times 10^{+07}$	0.88	2.00		
	6	373	$1.4 \times 10^{+18}$	2.38	2.00		
HAP/Gd (1 m%)	1	119	$3.6 \times 10^{+10}$	0.86	2.00	1.58	0.020
	2	170	$2.6 \times 10^{+08}$	0.79	1.03		
	3	194	$5.3 \times 10^{+11}$	1.14	1.56		
	4	215	$6.7 \times 10^{+08}$	0.92	2.00		
	5	394	$6.7 \times 10^{+03}$	0.66	2.00		
HAP/La (1 m%)	1	107	$1.5 \times 10^{+10}$	0.81	2.00	2.14	0.029
	2	149	$1.5 \times 10^{+08}$	0.74	1.43		
	3	186	$7.7 \times 10^{+11}$	1.13	2.00		
	4	196	$5.0 \times 10^{+12}$	1.23	1.16		
	5	208	$1.5 \times 10^{+13}$	1.31	2.00		
	6	303	$5.9 \times 10^{+05}$	0.76	1.00		
	7	352	$8.5 \times 10^{+10}$	1.44	2.00		
	8	389	$1.0 \times 10^{+18}$	2.43	1.22		

process of $CaSO_4$/Dy. They mentioned that the TL results clearly show that the absence of Dy removes the dosimetric peak near 220 °C in this material which is observed in our work, as well. Only Dy impurity develops the appropriate centers needed for observation of these peaks. These results emphasize the importance of Dy impurities in stabilizing the TL process needed to observe the dosimetric peak in this system [28, 29].

3.4 Effect of dopant percentages

In this stage, the different concentration of Dy, Eu, and Gd dopants within the range 0.5–2 m%, 1–4 m%, and 1–10 m% has been investigated, respectively. Due to the very low TL response of the La (1 m%), and also the nearly the same response as Gd (1 m%), only La (1 m%) sample result is used and compared to others. According to Fig. 10a, all the TL responses of the HAP-doped samples were saturated at doses of ~ 400 Gy or ~ 800 Gy. But, the sensitivity of the HAP/Eu (4 m%), HAP/Eu (5 m%), and HAP/Gd (10 m%) is more than the undoped HAP sample at the doses under ~ 400 Gy. On the other hand, Fig. 10b

shows the dramatic increase in TL responses of the HAP-doped Dy, especially for HAP/Dy (1 m%) in comparison with the undoped HAP, which is in agreement with our previous research work [8]. The results show an acceptable dose–response over the studied dose range for all the Dy-doped samples. The TL response of the HAP-doped Dy (1 m%) is at least ~ 12, ~ 30, and ~ 2 times greater than the undoped, Dy (0.5 m%), and Dy (2 m%) doped samples, respectively.

3.5 Fading

Stability of TL signal at room temperature is an important factor in radiation dosimetry. The loss in TL signal may occur due to heat, light, or any other means with respect to time. Thermal fading of the nanostructured HAP doped 1 m% of the different dopants and irradiated at 800 Gy and stored in dark place was investigated, and the results are demonstrated in Fig. 11. Accordingly, the fading rate of the HAP doped with Dy (1 m%), Eu (1 m%), Gd (1 m%), and La (1 m%) samples is ~ 5%, 30%, 40%, and 70% during 30 days, respectively. The approximate time to occur the
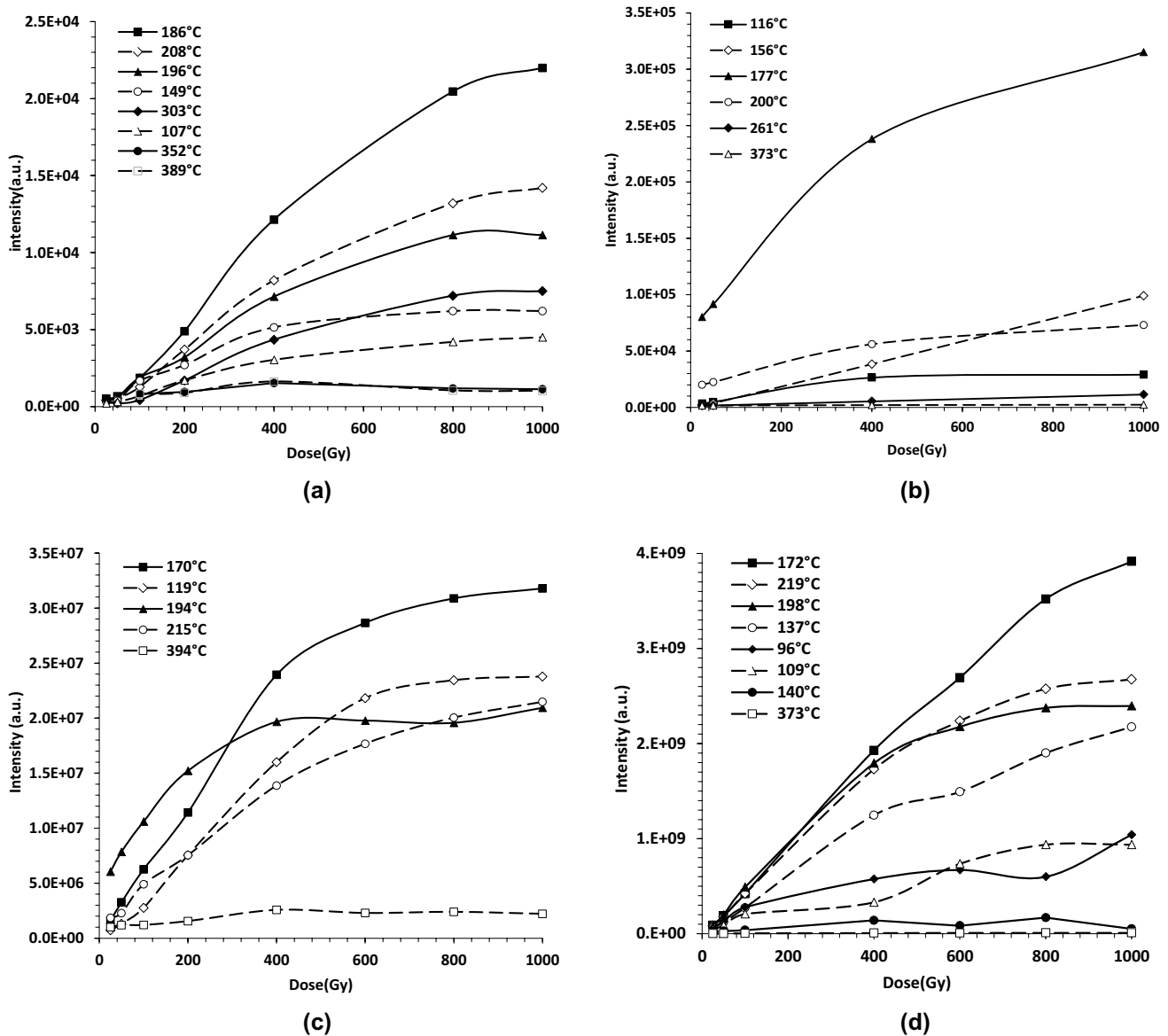
Fig. 8 Dose–response of deconvoluted peaks in 1 m% dopants of **a** La, **b** Eu, **c** Gd, and **d** Dy

fading in TL responses is mostly ~ 1 day for all the samples. Nevertheless, this rate almost remains constant for HAP/Dy, while continues up to ~ 7 days for the others. This is due to the fact of the shallow trap recombination, which is at 96 °C and 109 °C for HAP/Dy, and 107 °C, 116 °C, and 119 °C for HAP/La, HAP/Eu, and HAP/Gd, respectively, according to the deconvoluted glow curves depicted in Fig. 7. It is clear that the lowest temperature occurs in the lowest time. But for HAP/Dy sample, the result shows more stable in comparison with the others. This could be due to the intensity of the deeper peaks of the deconvoluted for each sample. On the other words, the deeper peaks make an important role in the stability of the TL response of the samples. According to Fig. 8, for HAP/Dy sample, the peaks

formed in 172 °C, 219 °C, 198 °C, and 137 °C have the same and main contribution in its TL intensity in different doses, respectively. Whereas, for HAP/Gd, the main peak in 194 °C has the main contribution in the TL response at doses lower than ~ 400 Gy. After this dose, the contribution of the peaks at 170 °C and 119 °C became dominant. In HAP/Eu, the mostly contribution belongs to the main peak at 177 °C. Therefore, the four deepest peaks in HAP/Dy have the same effect keeping the response stability via time, but in other samples, the number of deep peaks that simultaneously affects the stability of the TL response is comparably lower. Figure 12 shows an example of TL glow curves change via time for the HAP/Dy (1 m%). The peak height almost remains constant after different storage time, but
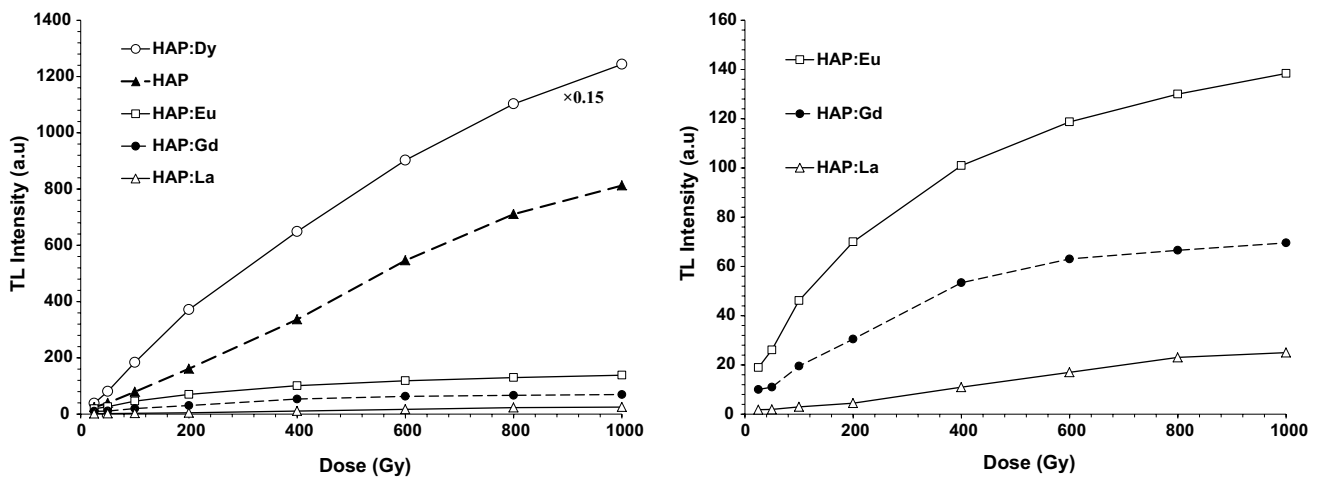
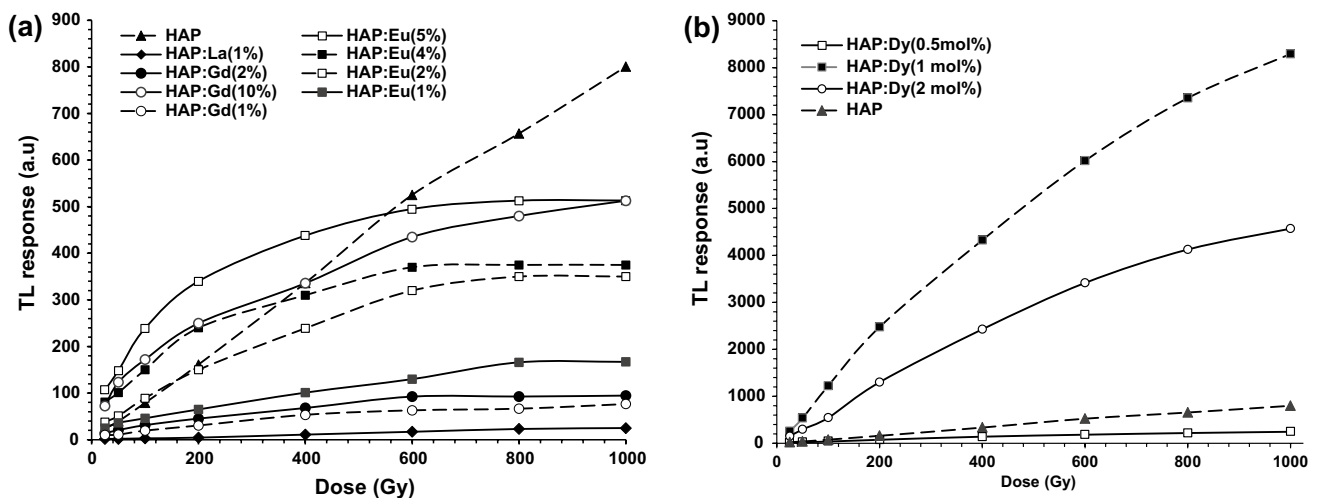**Fig. 9** Dose–response comparison of the HAP containing 1 m% of the dopants


Fig. 10 TL responses of the HAP doped with different dopants concentrations in comparison with the undoped HAP sample. **a** La, Gd, and Eu, **b** Dy

the total response, glow curve peak area, is changing drastically. This is why the authors choose the peak height as the TL response of the investigated samples. This figure demonstrates the effect of main peak intensity on the fading of the TL response as well.

4 Conclusion

Nanostructured HAP containing any one of the lanthanide elements, such as La, Eu, Gd, and Dy, was synthesized through hydrolysis method, and the XRD results confirmed the peaks according to the standard cards of HAP. The TL sensitivity of HAP can be further enhanced by doping with certain amount of impurities in an optimum

concentration. These impurity ions introduce allowed energy states (traps) in the forbidden energy gap of HAP to store the charges produced during irradiation. Subsequently, by heating the material after irradiation, these charges are released from the traps and recombine to give thermoluminescence. The preparation method affects significantly on thermoluminescence parameters. In this method of synthesis, doping of Eu, La, and Gd does not have significant effects on the TL intensities; however, peak positions have minor shifts. The most intense TL response was observed in the case of HAP doped 1 m% of Dy. In all the samples, the TL intensities faded after 1 day, but the rate of the fading shows increasing for the HAP doped Dy, Eu, Gd, and La samples, respectively. Therefore, the dose–response results indicate that the HAP/Dy sample
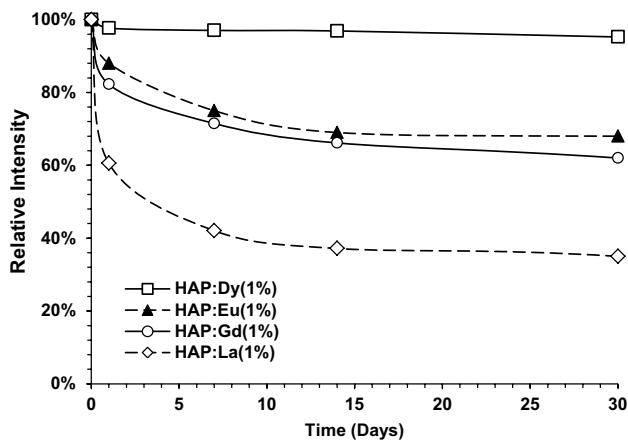
Fig. 11 Fading of HAP doped 1 m% of the different dopants and irradiated at 800 Gy
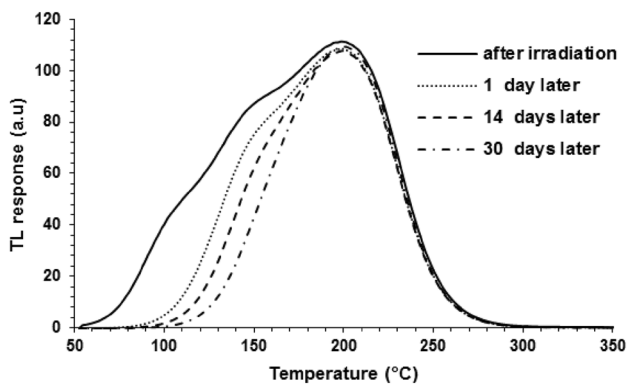
Fig. 12 TL glow curve of HAP/Dy (1 m%) after different storage times

could be used as a reliable dosimeter for the studied dose range. The Tm–Tstop method, as well as the TLanal program, shows its usefulness to calculate the kinetics parameters of TL produced samples, and it is helpful to discuss the fading phenomenon in TL materials.

Compliance with ethical standards

Conflict of interest The authors declare that they have no conflict of interest.

References

1. Chen R, McKeever SW (1997) Theory of thermoluminescence and related phenomena. World Scientific, Singapore
2. Furetta C, Weng P-S (1998) Operational thermoluminescence dosimetry. World Scientific Publishing Company, Singapore
3. Shafaei M, Ziaie F, Sardari D, Larijani M (2015) Study on carbonated hydroxyapatite as a thermoluminescence dosimeter. Kerntechnik 80:66–69
4. Zarinfar A, Shafaei M, Ziaie F (2015) Synthesis, characterization and thermoluminescence properties of nano-structure gadolinium doped hydroxyapatite (HAP: Gd). Proc Mater Sci 11:293–298
5. Chapman M, Miller A, Stoebe T (1979) Thermoluminescence in hydroxyapatite. Med Phys 6:494–499
6. Fukuda Y, Ohtaki H, Tomita A, Takeuchi N (1993) Thermoluminescence of hydroxyapatite doped with copper. Radiat Prot Dosim 47:205–207
7. Oliveira L, Rossi A, Baffa O (2012) A comparative thermoluminescence and electron spin resonance study of synthetic carbonated A-type hydroxyapatite. Appl Radiat Isot 70:533–537
8. Ziaie F, Farhadi Moein N, Shafaei M (2014) Thermoluminescent characteristics of nano-structure hydroxyapatite: Dy. Kerntechnik 79:500–503
9. Zarate-Medina J, Sandoval-Cedeño K, Barrera-Villatoro A, Lemus-Ruiz J, Rivera_Montalvo T (2015) Thermal effect on thermoluminescence response of hydroxyapatite. Appl Radiat Isot 100:50–54
10. Shafaei M, Ziaie F, Sardari D, Larijani M (2016) Thermoluminescence properties of gamma-irradiated nano-structure hydroxyapatite. Luminescence 31:223–228
11. Roveri N, Iafisco M (2010) Evolving application of biomimetic nanostructured hydroxyapatite. Nanotechnol Sci Appl 3:107
12. Alvarez R, Rivera T, Guzman J, Piña-Barba M, Azorin J (2014) Thermoluminescent characteristics of synthetic hydroxyapatite (SHAp). Appl Radiat Isot 83:192–195
13. Shih W-J, Chen Y-F, Wang M-C, Hon M-H (2004) Crystal growth and morphology of the nano-sized hydroxyapatite powders synthesized from $CaHPO_4 \cdot 2H_2O$ and $CaCO_3$ by hydrolysis method. J Cryst Growth 270:211–218
14. Mendoza-Anaya D, Flores-Díaz E, Mondragón-Galicia G, Fernández-García M, Salinas-Rodriguez E, Karthik T et al (2018) The role of Eu on the thermoluminescence induced by gamma radiation in nano hydroxyapatite. J Mater Sci Mater Electron 29:15579–15586
15. Madhukumar K, Varma H, Komath M, Elias T, Padmanabhan V, Nair C (2007) Photoluminescence and thermoluminescence properties of tricalcium phosphate phosphors doped with dysprosium and europium. Bull Mater Sci 30:527–534
16. Ravindranadh K, Babu B, Rao M, Shim J, Reddy CV, Ravikumar R (2015) Structural and photoluminescence studies of Co^{2+} doped Ca–Li hydroxyapatite nanopowders. J Mater Sci Mater Electron 26:6667–6675
17. Seth P, Aggarwal S, Rao S (2012) Thermoluminescence study of rare earth ion (Dy^{3+}) doped LiF:Mg crystals grown by EFG technique. J Rare Earths 30:641–646
18. Chung K, Lee J, Kim J (2012) A computer program for the deconvolution of the thermoluminescence glow curves by employing the interactive trap model. Radiat Meas 47:766–769
19. Manhas M, Kumar V, Ntwaeaborwa O, Swart H (2015) Photoluminescence and thermoluminescence investigations of $Ca_3B_2O_6$:Sm^{3+} phosphor. Mater Res Express 2:075008
20. Shafaei M, Ziaiedoustan A, Ziaie F, Rahmanifard R (2016) Study on thermoluminescence properties of europium doped nano-structure hydroxyapatite. IJRSM 4:47–51
21. Furetta C (2010) Handbook of thermoluminescence. World Scientific, Singapore
22. Rasheedy MS (1993) On the general-order kinetics of the thermoluminescence glow peak. J Phys Condens Matter 5:633
23. Gómez Ros JM, Kitis G (2002) Computerised glow curve deconvolution using general and mixed order kinetics. Radiat Prot Dosim 101:47–52

24. Vejnović Z, Pavlović MB, Ristić D, Davidović M (1998) On the general-order kinetics of the thermoluminescence glow peak and the calculation of parameters from glow curves. J Lumin 78:279–287

25. Noto LL (2014) Persistent luminescence mechanism of tantalite phosphors. University of the Free State, Bloemfontein

26. Puust L, Kiisk V, Utt K, Mändar H, Sildos I (2014) Afterglow and thermoluminescence of ZrO_2 nanopowders. Cent Eur J Phys 12:415–420

27. Mokoena P, Chithambo M, Kumar V, Swart H, Ntwaeaborwa O (2015) Thermoluminescence of calcium phosphate co-doped with gadolinium and praseodymium. Radiat Meas 77:26–33

28. Morgan M, Stoebe T (1990) Role of Dy in the thermoluminescence of CaSO4: Dy. Radiat Prot Dosim 33:31–33

29. Azorin J, González G, Gutierrez A, Salvi R (1984) Preparation and dosimetric properties of a highly sensitive $CaSO_4$:Dy thermoluminescent dosimeter. Health Phys 46:269–274